Mon. Not. R. Astron. Soc. **000**, 000–000 (0000) Printed 30 October 2014 (MN LATEX style file v2.2)

About the impact of baryons on the cluster mass function: Fitting formula and cosmological implications

Sebastian, Alex, Klaus and whoever is interested

30 October 2014

ABSTRACT

Galaxy cluster surveys allow to place tight constraints on key cosmological parameters and to improve our knowledge about dark energy. In order to fully exploit current and next-generation cluster samples it is of crucial importance to rely on an accurately calibrated cluster mass function. Typically, the calibration is done against large N-body simulations, taking only dark matter into account. We use the hydrodynamical Magneticum simulations to quantify the impact baryons have on the cluster mass function. Including baryonic effects leads to...

Key words: cosmology: theory - cosmology: cosmological parameters

1 INTRODUCTION

Galaxy clusters are the largest collapsed objects in the Universe. Their distribution in mass and redshift is highly sensitive to key cosmological parameters such as the matter density $\Omega_{\rm m}$, or the amount of matter fluctuations in the Universe σ_8. Furthermore, they can be used to constrain different models of dark energy as well the neutrino sector. Large cluster surveys have therefore proven as useful cosmological probes (e.g. Vikhlinin et al. 2009; Mantz et al. 2010; Rozo et al. 2010; et al. 2013; Planck Collaboration et al. 2013; Bocquet et al. 2014).

In all these analyses, the observed abundance of galaxy clusters is linked to the linear matter power spectrum through the cluster mass function, which can be estimated through an analytical approach (Press & Schechter 1974) or calibrated against numerical simulations. Tinker et al. (2008) use a set of large N-body simulations to provide a calibrated fitting function. While their mass function has established as the standard reference which is used in most cosmological analyses, the literature offers several alternatives (e.g. Jenkins et al. 2001; White et al. 2002; Warren et al. 2006; Watson et al. 2013). All these mass functions are comparable, and Planck Collaboration et al. (2013) show that their cosmological constraints are basically insensitive to the adopted mass function.

However, all mass functions obtained from N-body simulations suffer from the simplification of neglecting the baryonic component of the clusters. The pressure in the baryonic gas effectively leads to lower-mass clusters, and a decrease of the expected cluster abundance. Recently, various authors have investigated the baryonic impact on the cluster mass function (e.g. Cusworth et al. 2014). However, many of these works suffer from too simplistic modeling of the baryonic gas in the numerical simulations. Some of these simplifications are pre-heating at high redshift, negligence of radiative cooling or the baryons' self-gravity, and many other (probably cite something). Nevertheless, these studies suggest that baryonic dynamics do have an appreciable impact on the cluster mass function, by lowering the overall abundance of clusters by about 15% Cusworth et al. (2014).

In this work, we analyze a simulated cluster sample generated by the Magneticum simulations (Dolag K. et al. 2014). These are a set of hydrodynamical simulations covering large cosmological volumes for a variety of resolutions. We use these data to calibrate a cluster mass function that takes into account baryonic effects. This paper is organized as follows: In Section 2 we present the Magneticum simulations and the cluster sample used for this work. In Section 3 we introduce our analysis method used to perform the fit, and show how we tested it for potential biases. We present our fit results in Section 4 and disucss the cosmological impact in Section 5.

We will consider different mass definitions: (1) virial mass $M_{\rm vir}$, which is calculated by integrating out to the cluster's virial radius, (2) "mean overdensity" mass (e.g. $M_{200,\,\rm mean}$), which is the mass enclosed within a sphere of radius $r_{200,\,\rm mean}$, in which the mean matter density is equal to X times the Universe's mean density at the cluster's redshift, and (3) "critical overdensity" mass (e.g. $M_{500,\,\rm crit}$), which is analogous to (2) but with respect to the critical density. The critical density at the cluster's redshift is $\rho_{\rm crit}(z) = 3H^2(z)/8\pi G$, where $H(z)$ is the Hubble parameter; the mean matter density is $\bar{\rho}_{\rm m}(z) = \Omega_{\rm m}(z)\rho_{\rm crit}(z)$.

2 SIMULATIONS AND CLUSTER SELECTION

2.1 The Magneticum Simulations

This Section will need some input from Klaus. Introduce the hydrosims and tell why they are so incredibly awesome. We also ran some DM simulations for comparison.

All simulations are carried out assuming a spatially flat ΛCDM cosmology with matter density $\Omega_m = 0.272$, baryon den-

Table 1. Mass function parameters from our dark matter simulations, our hydro simulations, and from the literature (Tinker et al. 2008). Cluster masses are defined with respect to $M_{200,\mathrm{mean}}$.

Parameter	A	a	b	c	A_z	a_z	b_z
DM	0.223 ± 0.024	1.69 ± 0.10	2.05 ± 0.23	1.242 ± 0.028	-0.25 ± 0.35	0.091 ± 0.088	-0.02 ± 0.31
hydro	0.282 ± 0.035	2.14 ± 0.18	1.54 ± 0.14	1.319 ± 0.039	-0.38 ± 0.33	0.022 ± 0.072	0.08 ± 0.21
Tinker et al. (2008)	0.186	1.47	2.57	1.19	-0.14	-0.06	0.011

sity $\Omega_b = 0.0456$, variance in the matter field[1] $\sigma_8 = 0.809$, and Hubble constant $H_0 = 70.4$.

2.2 Halo Selection

This Section needs input from Alex who actually produced the catalogs. Also mention that we chose a rather large number of particles for the haloes in the hydro simulations. Not sure if we explicitly mention the convergence problems we observed otherwise.

3 ANALYSIS METHOD

We provide the theoretical background on the cluster mass function and introduce its functional form. We then present the method used to perform the multi-dimensional fits used to extract the mass function parameters from our simulations.

3.1 The Cluster Mass Function

The number density of galaxy clusters with respect to mass M is

$$\frac{dn}{dM} = f(\sigma)\frac{\bar{\rho}_\mathrm{m}}{M}\frac{d\ln\sigma^{-1}}{dM}, \quad (1)$$

with the mean matter density $\bar{\rho}_\mathrm{m}$ (at redshift $z = 0$), and

$$\sigma(M,z) = \frac{1}{2\pi^2}\int P(k,z)\hat{W}^2(kR)k^2dk, \quad (2)$$

the variance of the matter density field $P(k,z)$ smoothed with the Fourier transform $\hat{W}$ of the real-space top-hat window function of radius $R = (3M/4\pi\bar{\rho}_\mathrm{m})^{1/3}$. The function $f(\sigma)$ is assumed to be universal, i.e. independent of cosmology, and is commonly parametrized as

$$f(\sigma) = A\left[\left(\frac{\sigma}{b}\right)^{-a} + 1\right]\exp\left(-\frac{c}{\sigma^2}\right) \quad (3)$$

with four parameters A, a, b, c that need to be calibrated. Here, A sets the overall normalization, a and b are the slope and normalization of the low-mass power law, and c sets the scale of the high-mass exponential cutoff (analogous to e.g. Tinker et al. 2008).

If working with the virial mass definition M_vir, the function $f(\sigma)$ is indeed expected to be universal. However, when using other definition with respect to mean or critical density, this universality will no longer hold, and we parametrized a possible redshift dependence as a power law of $1 + z$:

$$A(z) = A_0(1+z)^{-A_z} \quad (4)$$

$$a(z) = a_0(1+z)^{-a_z} \quad (5)$$

$$b(z) = b_0(1+z)^{-b_z} \quad (6)$$

where the subscript 0 denotes the values at redshift $z = 0$, and where A_z, a_z, b_z are additional fit parameters. The cutoff scale c is a constant. Note that the cluster number density depends on redshift through $\sigma(M,z)$ and the explicit redshift dependence of $f(\sigma)$.

3.2 Parameter Estimation

When fitting for the mass function, we are facing a problem with moderately large dimensionality (7 parameters) and utilize the `emcee`[2] code for efficient exploration of parameter space (Foreman-Mackey et al. 2013). The likelihood of each point in parameter space $\boldsymbol{p}$ is calculated in the following way: We calculate the matter power spectrum using the transfer function by Eisenstein & Hu (1998, 1999) as this is the prescription used to set up the initial conditions of the Magneticum simulations. Then, for each redshift, we calculate the mass function following Equations 1-3. We apply a binning to the data that is equally distributed in log-space with $\Delta\log_{10} M = 0.01$. We checked that decreasing the bin size does not change our results. Finally, we evaluate the likelihood $\mathcal{L}$ by applying the Cash statistics (Cash 1979), which is an application of Poisson statistics

$$\ln\mathcal{L} = \sum_i \ln\frac{dn(M_i|\boldsymbol{p},z)}{d\log M}\Delta\log M - \int\frac{dn(M|\boldsymbol{p},z)}{dM}dM, \quad (7)$$

where i runs over all clusters in the sample. Note that the second term equals the total number of expected clusters.

In practice, given a set of fit parameters $\boldsymbol{p}$, we perform the above calculation for each snapshot redshift and for each of the simulation's boxes separately, sum the log-likelihoods, and return the result to `emcee`.

We tested our fitting procedure against several mock catalogs that contain a factor 100 times more clusters than our data. We recovered the input values within the uncertainties and conclude that our fitting method is unbiased to a level that is much smaller than the errors we report.

4 RESULTS

We use the fitting method described above to perform mass function fits against our hydro and DM simulation samples. We compare our results to previous studies. We present our mass function for $M_{500,\,\mathrm{crit}}$ in Section 4.2.

4.1 Mass function fits and comparison with other studies

Figure 2 shows our main results. We show the data points for the DM and hydro simulations as well as our best fit mass functions for both sets of simulations. The DM simulations are in good agreement with the fitting formula by Tinker et al. (2008), while it is clear that the hydro simulations predict less massive clusters. For redshifts smaller than about 1, we expect about 10% less clusters

[1] See Equation 2 for the exact definition

[2] http://dan.iel.fm/emcee/current

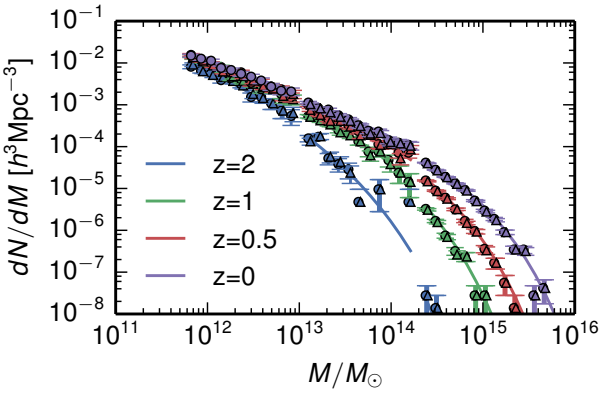

Figure 1. Mass function dN/dM at four different redshifts. The round symbols correspond to the DM simulations, and triangles correspond to the hydro simulations. The mass function from Tinker et al. (2008) is indicated by the solid lines. Note that our fits are not distinguishable from their fit in such a figure given its large dynamic range.

from the hydro simulations. Note however that the error bars are quite large, and the 2σ regions shown in Figure 2 still overlap.

In Table 1 we present the fit parameters obtained from our DM and hydro mass functions. Masses are defined as $M_{200,m}$. The corresponding covariance matrices are presented in Table **??**.

- Present the overall goodness of the fits (χ^2).
- Same thing for each redshift, i.e. test whether the redshift evolution is adequately parametrized.

4.2 Mass function for $M_{500,\,\mathrm{crit}}$

In cluster cosmology, the most commonly used mass definition is $M_{500,\,\mathrm{crit}}$. The choice of this definition is due to the fact that it represents the best regime for X-ray observations. Using a cluster catalog extracted from our hydro simulations using this mass definition, we repeat the analysis described above, and fit for the mass function parameters. Our results are presented in Table 2.

The tabled values can directly be used for any cluster study that uses the same mass definition. Blabla some statement about whether or not the use the covariance matrix will change cosmological results.

5 COSMOLOGICAL IMPACT

We discuss how our findings from Section 4 affect cluster cosmology, and show how the use of a different mass function affects constraints in the Ω_m-σ_8 plane. We analyze our hydro sample, assuming the three different mass function considered so far. In Table 3 and Figure 4 we show how the use of a non-hydro mass function leads to an underestimation of Ω_m by about $\Delta\Omega_\mathrm{m} \approx -0.01$.

- Interestingly, our hydro and the Tinker MF give identical constraints on σ_8, and our DM prefer a slightly higher value.
- Compare this shift to current (and future?) constraints.
- How does it affect the cluster vs. CMB tension?

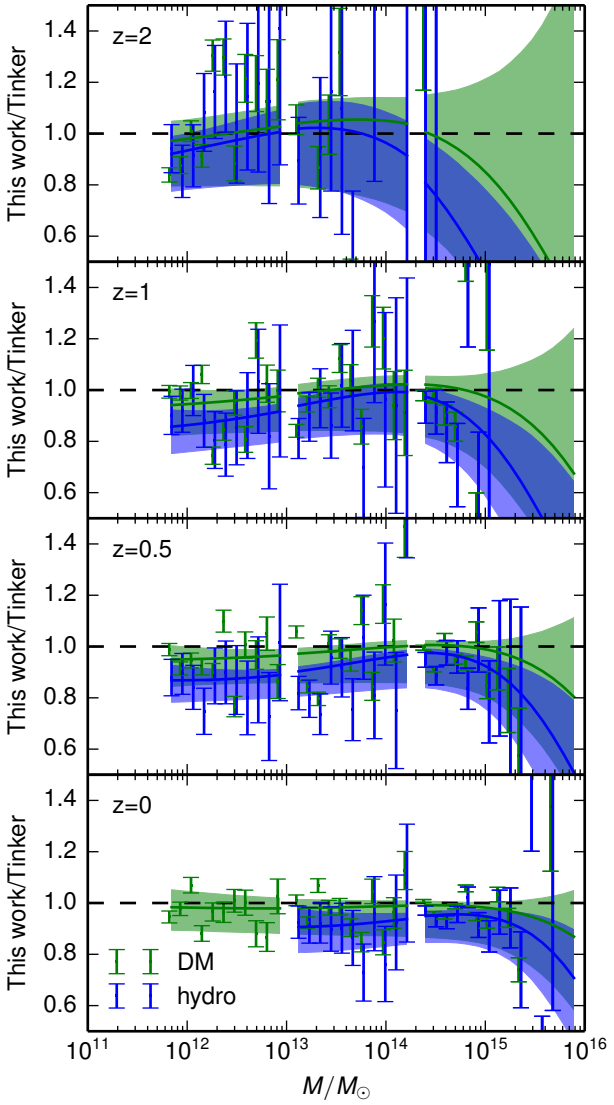

Figure 2. Relative difference between our simulations (DM in green, hydro in blue) and the Tinker fit. The data points are slightly offset in mass direction for better readability. The solid lines correspond to the best fit; the colored regions correspond to the area enclosed within the 5th and 95th percentile (roughly the 2σ region).

Table 3. Cosmological constraints for different mass functions.

Parameter	Ω_m	σ_8	$\sigma_8(\Omega_\mathrm{m}/0.27)^{0.3}$
Input	0.272	0.809	(0.8108)
hydro	0.273 ± 0.002	0.808 ± 0.003	0.8108 ± 0.0016
DM	0.264 ± 0.002	0.811 ± 0.003	0.8058 ± 0.0017
Tinker08	0.263 ± 0.003	0.809 ± 0.003	0.8021 ± 0.0018

6 OPTIMAL MASS DEFINITION

- We want to show what mass definition is "ideal" in the sense that cosmological constraints are the tightest.
- Perform the mass function fit and cosmological analysis for each definition available, and compare the area enclosed in Ω_m-σ_8 space.
- From this, choose the "best" definition.

Table 2. Mass function parameters obtained from our hydro simulation for the mass definition $M_{500,\,\mathrm{crit}}$. We also provide the full covariance matrix.

Param.	A	a	b	c	A_z	a_z	b_z
mean	0.15 ± 0.02	1.71 ± 0.21	2.15 ± 0.32	1.86 ± 0.07	0.70 ± 0.16	0.84 ± 0.06	-0.60 ± 0.09
Covariance matrix							
A	4.53×10^{-4}	1.18×10^{-3}	-4.03×10^{-3}	1.06×10^{-4}	-7.55×10^{-4}	-1.75×10^{-4}	7.20×10^{-4}
a		9.87×10^{-3}	-1.35×10^{-2}	2.08×10^{-3}	3.64×10^{-3}	2.38×10^{-4}	-2.25×10^{-3}
b			3.99×10^{-2}	-1.05×10^{-3}	-7.62×10^{-4}	2.59×10^{-3}	-2.23×10^{-3}
c				7.71×10^{-4}	-8.43×10^{-5}	7.71×10^{-4}	-4.18×10^{-4}
A_z					1.05×10^{-1}	1.24×10^{-2}	-8.65×10^{-2}
a_z						6.43×10^{-3}	-1.46×10^{-2}
b_z							7.60×10^{-2}

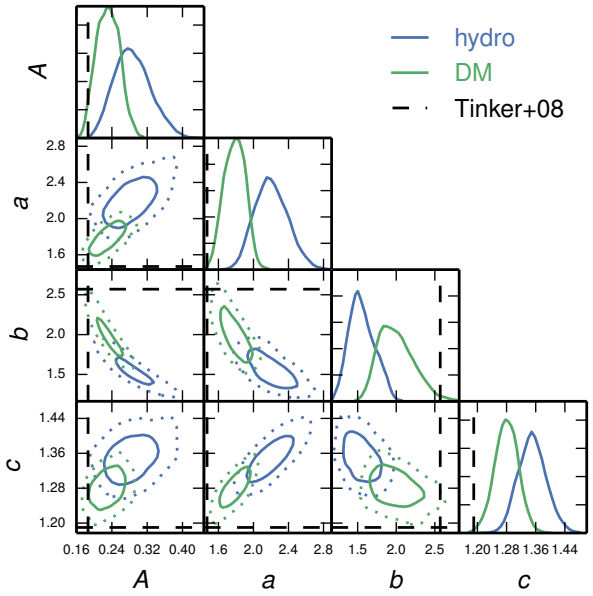

Figure 3. Parameter estimates for our dark matter simulation (green) and hydro simulation (blue). The results are marginalized over the parameters' redshift dependence (Equations 4-6). The fit from Tinker et al. (2008) is indicated by the dashed lines.

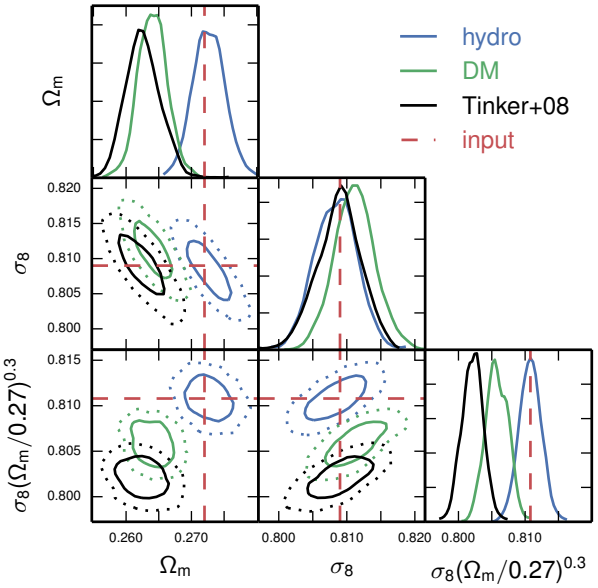

Figure 4. Likelihood contours (68% and 95% confidence) in Ω_m-σ_8 space for the analysis of the cluster sample extracted from our hydro simulation. We used the Tinker et al. (2008) mass function (black), the mass function obtained from our DM simulations (green) and from our hydro simulations (blue). The simulation input values are marked by the red lines, and are perfectly recovered using the MF from our hydro simulations.

• Comment in light of feasibility, and different mass measurement techniques (X-ray, dispersion, WL, richness?).

7 SUMMARY

Review our results. Point our that these kind of studies are crucial for the next-generation cluster surveys.

ACKNOWLEDGMENTS

We acknowledge the support of the DFG Cluster of Excellence "Origin and Structure of the Universe" and the Transregio program TR33 "The Dark Universe".

REFERENCES

Bocquet et al. 2014, ArXiv e-prints
Cash W., 1979, ApJ, 228, 939
Cusworth S. J., Kay S. T., Battye R. A., Thomas P. A., 2014, MNRAS, 439, 2485
Dolag K. et al. 2014, In Preparation
Eisenstein D. J., Hu W., 1998, ApJ, 496, 605
Eisenstein D. J., Hu W., 1999, ApJ, 511, 5
et al. B., 2013, ApJ, 763, 147
Foreman-Mackey D., Hogg D. W., Lang D., Goodman J., 2013, PASP, 125, 306
Jenkins A., Frenk C. S., White S. D. M., Colberg J. M., Cole S., Evrard A. E., Couchman H. M. P., Yoshida N., 2001, MNRAS, 321, 372
Mantz A., Allen S. W., Ebeling H., Rapetti D., Drlica-Wagner A., 2010, MNRAS, 406, 1773
Planck Collaboration Ade P. A. R., et al. 2013, ArXiv e-prints
Press W., Schechter P., 1974, ApJ, 187, 425
Rozo E., Wechsler R. H., Rykoff E. S., Annis J. T., Becker M. R., Evrard A. E., Frieman J. A., Hansen S. M., Hao J., Johnston D. E., Koester B. P., McKay T. A., Sheldon E. S., Weinberg D. H., 2010, ApJ, 708, 645

Tinker et al. 2008, ApJ, 688, 709
Vikhlinin A., Kravtsov A. V., Burenin R. A., Ebeling H., Forman W. R., Hornstrup A., Jones C., Murray S. S., Nagai D., Quintana H., Voevodkin A., 2009, ApJ, 692, 1060
Warren M. S., Abazajian K., Holz D. E., Teodoro L., 2006, ApJ, 646, 881
Watson W. A., Iliev I. T., D'Aloisio A., Knebe A., Shapiro P. R., Yepes G., 2013, MNRAS, 433, 1230
White M., Hernquist L., Springel V., 2002, ApJ, 579, 16